Available online at www.sciencedirect.com
SCIENCE DIRECT
Polymer 47 (2006) 6123–6130
polymer
www.elsevier.com/locate/polymer

ATR–FTIR studies of a thermo-responsive ABA triblock copolymer gelator in aqueous solution

Chris Sammon [a,*], Chengming Li [b], Steven P. Armes [b], Andrew L. Lewis [c]

[a] *Materials and Engineering Research Institute, Sheffield Hallam University, Sheffield, S1 1WB, UK*
[b] *Department of Chemistry, Dainton Building, University of Sheffield, Brook Hill, Sheffield, S3 7HK, UK*
[c] *Biocompatibles UK Ltd., Chapman House, Farnham Business Park, Weydon Lane, Farnham, Surrey, GU9 8QL, UK*

Received 13 March 2006; received in revised form 7 June 2006; accepted 9 June 2006
Available online 14 July 2006

Abstract

A variable temperature ATR–FTIR study of the gelation behaviour of a thermo-responsive ABA triblock copolymer (A = poly(*N*-isopropylacrylamide) and B = poly[2-(methacryloyloxy)ethyl phosphorylcholine]) is reported. Close inspection of selected copolymer and water bands in the temperature resolved spectra provides evidence for the dehydration of the poly(*N*-isopropylacrylamide) chains above a critical gelation temperature of approximately 37 °C, while the central poly[2-(methacryoyloxy)ethyl phosphorylcholine]) chains remain hydrated. A blue shift in the amide I peak and a red shift in the amide II band indicate a reduction in the hydrogen bonding between the PNIPAM amide functional group and the solvent water. This is corroborated by a decrease in the intensity of the amide I peak above the gel point. Evidence of hydrophobic interactions and an indication of the source of the gelation mechanism were observed in the form of a red shift in the antisymmetric CH vibration with increasing temperature. These findings are consistent with the formation of a micellar gel network by the copolymer chains.

Keywords: ATR–FTIR; Hydrogen bonding; Gelation

1. Introduction

Aqueous solutions of poly(*N*-isopropylacrylamide) (PNIPAM) exhibit a reversible thermal phase transition with a lower critical solution temperature (LCST) of ~32 °C for linear chains [1,2]. Hence PNIPAM is soluble at ambient temperature but precipitates from hot aqueous solution due to its coil-to-globule transition. This effect is exploited in the preparation of temperature-activated PNIPAM-based hydrogels for biomedical applications such as on/off drug release, the reversible attachment/detachment of cultured cells [3–6], and conferring biocompatibility onto various substrates [7,8].

The phosphorylcholine (PC) group is a structurally important motif within cell membranes, and it is well-documented that synthetic phosphorylcholine-based copolymers can be used to produce surface coatings that are remarkably resistant to protein adsorption and bacterial/cellular adhesion [9,10]. In particular, so-called 'biomimetic' monomers such as 2-(methacryloyloxy)ethyl phosphorylcholine [MPC] have received increasing attention, since its statistical copolymerization confers clinically-proven biocompatibility to a wide range of surface coatings and gels (see Refs. [9c,11]). Thermal and Raman spectroscopic studies by Ishihara et al. suggest that the excellent biocompatibility of MPC-based coatings is due to the strongly hydrophilic nature of the MPC monomer [12]. Recently Armes et al. showed that MPC is readily polymerized with reasonably good control using atom transfer radical polymerization (ATRP) [13]. This synthetic advance provides the opportunity to produce a wide range of new controlled-structure biocompatible diblock copolymers. Recently, Armes and co-workers described the synthesis of new *thermo-responsive* gelators based on PNIPAM–PMPC–PNIPAM triblock copolymers using this synthetic methodology [14]. These ABA-type triblock copolymers form micellar gel networks at

* Corresponding author. Tel.: +44 114 2253890.
E-mail address: c.sammon@shu.ac.uk (C. Sammon).

0032-3861/$ - see front matter © 2006 Elsevier Ltd. All rights reserved.
doi:10.1016/j.polymer.2006.06.013

physiologically relevant conditions, i.e. in phosphate buffered saline (PBS) solutions at pH 7.4 and 37 °C. The minimum copolymer concentration required for free-standing gels is around 6–7% by weight, and, since they contain more than 90% water, these gels are relatively soft. Nevertheless, cell viability studies confirmed that these gels are sufficiently biocompatible to allow V79 hamster lung cells to be cultured *in situ*, indicating very low or zero cytotoxicities.

ATR–FTIR is a very important tool for characterising hydrogen bonding in aqueous systems (for examples see Refs. [15–17]) and determining the interactions of adsorbed and absorbed water with polymer matrices (for examples see [18–21]). The detailed theory of attenuated total reflectance Fourier transformed infrared spectroscopy (ATR–FTIR) is available elsewhere [22] but it is worth highlighting the salient points that are pertinent to this paper. The key feature of the ATR experiment is the character of the evanescent field, which develops during the reflection of radiation at the interface of a material with a high refractive index (ATR crystal, n_2) and a material with a low refractive index (sample, n_1). Attenuation of the evanescent field by functional groups in the sample results in a spectrum that is analogous to an absorption spectrum. The depth of penetration (dp) of the evanescent field is governed by the wavelength of incident radiation in the high refractive index medium (λ_1), the angle of incidence (θ_{inc}) and the ratio of the sample and ATR crystal refractive indices (n_{21}). This limits the sampling depth, which can be approximated using Eq. (1). In practice, the effective sampling depth is considered to be ~3dp.

$$\mathrm{dp} = \frac{\lambda_1}{2\pi\left(\sin^2\theta_{inc} - n_{21}^2\right)^{1/2}} \quad (1)$$

As a result, the spectral information collected will only be representative of the first few microns that are close to the ATR crystal sample interface, regardless of the overall thickness of the sample. Therefore it is possible to obtain spectra from very strongly absorbing materials, including water. Infrared spectroscopy has been used to characterise the gel structure of a number of systems, examples include cellulose ethers [23,24], proteins [25,26], starches [27–30] and synthetic polymers [31–35].

Su et al. used transmission FTIR to study the association behaviour of PEO–PPO–PEO block copolymers in both aqueous solution [32] and organic solvents [33]. They observed systematic changes in the position and shape of antisymmetric ν(CH), methyl deformation and C–O–C vibrations in the solution and gel states. They attributed these changes to differences in the hydration properties and hydrophobic interactions of the non-polar groups in the triblock copolymer at different molecular weights.

Maeda et al. examined the changes in the hydration states of aqueous solutions of two different polyacrylamides during the coil–globule transition using transmission FTIR [34,35]. D_2O was used to avoid overlap between the amide I band of the acrylamide and the δ(OH) band due to water. Two distinct amide species could be distinguished: amide hydrogen-bonded to sorbed water and amide hydrogen-bonded to neighbouring acrylamide NH groups. Red shifts in the frequencies of ν(CH) groups were observed during gelation and these changes were the result of attractive methyl–methyl ('hydrophobic') interactions brought about by dehydration of the polymer. Metal halide salts reduced the critical gelation temperature but had no effect on the shape of the bands associated with the polymer in its hydrated or dehydrated state. Unfortunately, the long path length of the transmission cell that was utilized prevented the elucidation of any modifications to the water structure during gelation.

In the present work ATR–IR spectroscopy has been used to study the gelation behaviour of a thermo-responsive PNIPAM–PMPC–PNIPAM triblock copolymer in aqueous solution as a function of temperature. For copolymer concentrations above 6–7% (w/w), the critical gelation temperature of this copolymer is around 37 °C [14]. The aim of this work was to use a spectroscopic method to elucidate the molecular interactions that cause micellar network formation by probing the hydrogen bonding and hydrophobic interaction changes during thermal gelation.

2. Experimental

2.1. Polymer synthesis

The synthesis of the $NIPAM_{89}$–MPC_{250}–$NIPAM_{89}$ triblock copolymer gelator was carried out in two steps using the so-called 'macro-initiator' approach. In the first step, a bifunctional Br–MPC_{250}–Br macro-initiator was prepared as follows. MPC (3.72 g, 12.5 mmol) was polymerized in 5 ml methanol at 20 °C using standard Schlenk (i.e. oxygen free environment) techniques, diethyl *meso*-2,5-dibromoadipate as a bifunctional ATRP initiator (18 mg, 0.05 mmol, target degree of polymerization = 250) and a Cu(I)Br/2bpy catalyst (14.4 mg, 0.10 mmol Cu(I)Br; 31.2 mg, 0.20 mmol bpy). After 4 h, the MPC conversion was typically more than 98% as judged by ^{1}H NMR (disappearance of vinyl signals between δ 5.5 and 6.0). The reaction flask was immersed in liquid nitrogen to terminate this first-stage polymerization, excess methanol was added to the frozen solution and the resulting solution was then passed though a silica gel column [silica gel 60 (0.063–0.200 mm)] to remove the spent ATRP catalyst. After solvent evaporation, the solid polymer was dissolved in de-ionized water and freeze-dried overnight. The resulting bifunctional Br–MPC_{250}–Br macro-initiator was obtained as a white powder (3.3 g). Aqueous GPC studies indicated an M_n of approximately 39,000 and an M_w/M_n of around 1.32 versus poly(ethylene oxide) standards. The second-stage polymerization to produce the $NIPAM_{89}$–MPC_{250}–$NIPAM_{89}$ triblock copolymer was carried out as follows. *N*-Isopropylacrylamide (NIPAM; 1.13 g; 10 mmol) and Cu(I)Br/Me_4Cyclam catalyst (7.2 mg, 0.05 mmol Cu(I)Br; 12.8 mg, 0.05 mmol Me_4Cyclam) were added to 10 ml degassed methanol in a Schlenk flask and stirred in an ice bath to form an homogeneous solution under a nitrogen atmosphere. The Br–MPC_{250}–Br macro-initiator (1.84 g; 0.05 mmol

bromine) was degassed and added under a nitrogen atmosphere and the NIPAM polymerization was allowed to continue for 2 h until ^{1}H NMR analysis indicated no further change in conversion. The monomer conversion was calculated by comparing the vinyl signals between δ 5.5 and 6.0 to the single isopropyl proton signal using ^{1}H NMR spectroscopy (d_4-CD_3OD). Excess methanol was then added to dilute the reaction solution, which was passed through a silica gel column to remove the spent catalyst. After solvent evaporation, the isolated solid was dissolved in de-ionized water and any remaining NIPAM monomer was removed by ultrafiltration (membrane molar mass cut-off $= 10^4$ g mol^{-1}) until ^{1}H NMR analysis indicated the absence of any vinyl signals between δ 5.5 and 6.0. Finally, a white powder was obtained by freeze-drying overnight (2.3 g). The second-stage NIPAM polymerization is not well controlled and the PNIPAM chains are of relatively high polydispersity ($M_w/M_n > 1.50$) compared to the central PMPC block. Nevertheless, the final PNIPAM–PMPC–PNIPAM copolymer has a well-defined triblock architecture, which is essential for gelation behaviour [14] (Fig. 1).

2.2. ATR–FTIR measurements

ATR–FTIR spectra were collected using a temperature-controlled Golden Gate™ single reflection ATR accessory (SpectraTech) coupled to a ThermoNicolet Nexus FTIR spectrometer. Aqueous copolymer solutions (~9.6% w/w) were placed in direct contact with the ATR crystal and sealed using a 'volatile' cap to ensure no water loss during the heating and cooling runs. The samples were allowed to equilibrate for 8 min at the required temperature prior to data collection. Data were collected by averaging over 64 scans at 4 cm^{-1} resolution. Both the blank ATR crystal and 18 mΩ water were used as reference backgrounds under the same conditions. FTIR data were manipulated using Omnic v6.1A™ provided by ThermoNicolet. The band fitting was conducted in the Galactic GRAMS/32™ environment, using 100% Lorentzian line shapes and a linear baseline. Peak positions, peak intensities and band widths were all allowed to vary during the iterative fitting process and the default settings of the software minimisation process were used to determine the optimum fit of the synthetic spectrum to the real spectrum. For the generation of Fig. 6(a–e) the gelation measurements were run in triplicate from the *same* stock solution.

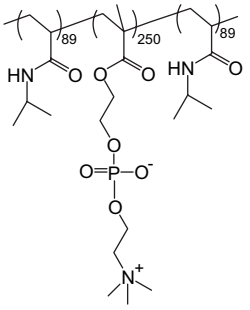

Fig. 1. Chemical structure of the thermo-responsive $PNIPAM_{89}$–$PMPC_{250}$–$PNIPAM_{89}$ triblock gelator used in this study.

3. Results and discussion

Variable temperature ATR–FTIR studies on 9.6% (w/w) aqueous solutions of PNIPAM–PMPC–PNIPAM triblock copolymers indicate that a number of reproducible spectral changes occur during gelation, see Fig. 2(a–c). All of the

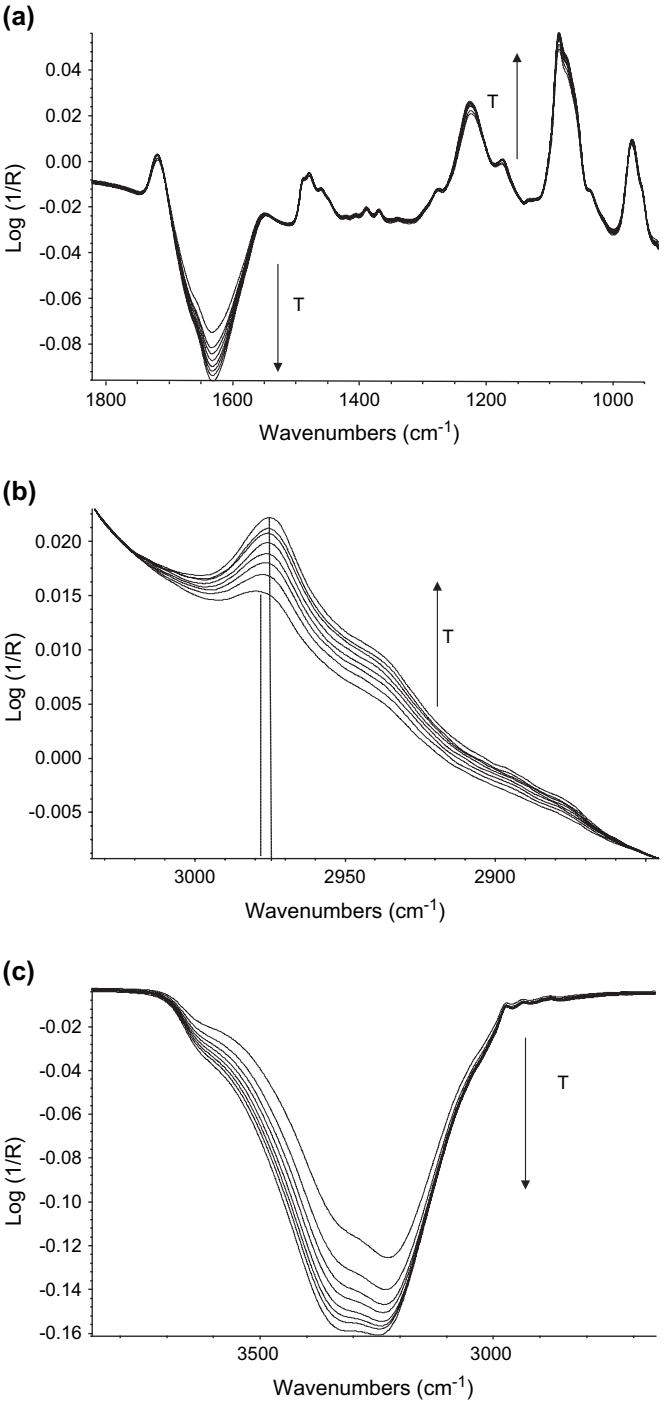

Fig. 2. (a) Plot of the fingerprint region obtained for the copolymer solution versus pure water at the same temperature; (b) plot of the ν_{as}(CH) obtained for the copolymer solution versus the clean ATR crystal at the same temperature; (c) plot of the ν(OH) obtained for the copolymer solution versus pure water at the same temperature (the arrows indicate increasing temperature from 30 °C to 44 °C).

single beam spectra of the aqueous copolymer shown in Fig. 2(a–c) were the result of the ratio of the single beam spectra of the copolymer solution and that of pure water at the same temperature so as to reduce the signal from the dominant water component. The main spectroscopic differences observed are changes in the intensities and positions of bands associated with the copolymer and water, which can be directly related to a redistribution of water molecules during gelation. These changes will be discussed in detail below. Fig. 2(a) shows the changes occurring in the so-called fingerprint region. There is a loss in intensity in the δ(OH) band ($\sim$1630 cm^{-1}) with increasing temperature as the hydrogen-bonded water is removed from the amide groups of the copolymer during the formation of the micellar network. There are also increases in the band intensities associated with functional groups on the copolymer chains; this is because the gel phase is denser than the aqueous copolymer solution. The gel therefore preferentially 'falls' into the evanescent field due to the horizontal configuration of the ATR experiment.

As the density of the gel increases and water is excluded from specific regions of the triblock system, the number of polymer–polymer hydrophobic interactions (i.e. attractive forces between hydrophobic groups) is expected to increase. Su et al. have shown that, for PPO–PEO block copolymers, the antisymmetric methyl stretch is particularly sensitive to hydrophobic interactions [32]. Fig. 2(b) shows the ν(CH) region of the copolymer solution during gelation and there is clear evidence of a red shift of $\sim$4–5 cm^{-1} in the ν_{as}(CH) region during the temperature ramp. This is a strong indication of increased attractive hydrophobic interactions between neighbouring copolymer chains and is almost certainly due to the closer proximity of methyl groups on the PNIPAM blocks as these chains reorganise to form a micellar network. The magnitude of the shift found in the present work is somewhat less than that observed by Su et al., who reported red shifts in the order of 10 cm^{-1}. Our smaller red shift may be due to 'weaker' relative gel strength, although this hypothesis is yet to be confirmed.

Information pertaining to the redistribution of the water molecules within the copolymer gel is also available from spectral changes in the ν(OH) region, see Fig. 2(c). It is known that in pure liquid water the shape of the ν(OH) band is sensitive to changes in temperature; lower intensities, a 'sharpening' of the broad band and a net shift to higher wavenumbers are observed as the temperature is increased. This has been attributed to a reduction in the average hydrogen bonding strength of water in the system [16,17,23]. For pure water these changes are clearly shown in Fig. 3(a): these data were acquired with the same instrument under the same conditions as those employed for the copolymer solution data. Fig. 3(b) shows the integrated areas of both the ν(OH) and δ(OH) bands as a function of temperature and was derived from the spectra shown in Fig. 3(a). The intensity of the ν(OH) band decreases linearly as the solution temperature is raised, while the δ(OH) band intensity is temperature-independent. Thus the lower intensity of the δ(OH) band shown in Fig. 2(a) must be due to water loss from the ATR/sample interface due to syneresis,

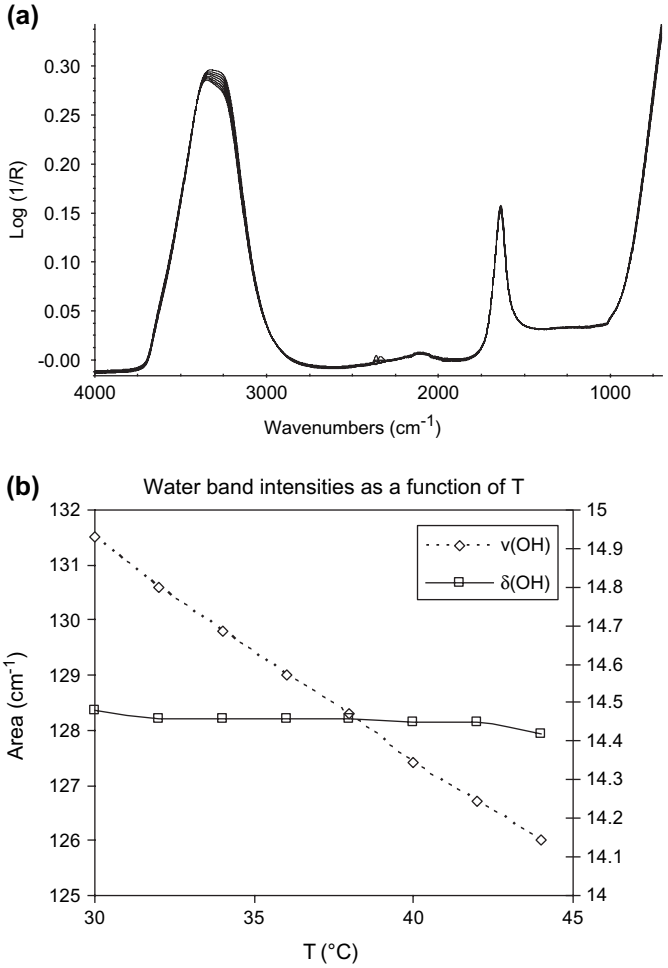

Fig. 3. (a) The ATR–FTIR spectra of pure liquid water between 30 and 44 °C at 2 °C intervals and (b) the corresponding integrated areas as a function of time for the ν(OH) and δ(OH) vibrations.

while the ν(OH) band shown in Fig. 2(c) is a combination of both water loss *and* changes in the hydrogen-bonded water network within the gel layer. Fig. 2(c) shows the changes to the intensity and shape of the ν(OH) region of the gel with pure water at the same temperature used as a background reference. Consideration of this complex band is required to understand the spectral changes that occur during gelation. The ν(OH) band of water can be considered to be made up of either a number of components (mixture model) or a continuum of water with different hydrogen bond angles and strengths (continuum model) [36,37]. In both cases a shift to higher wavenumber is associated with weaker hydrogen bonding whereas lower wavenumbers indicate stronger hydrogen bonding. According to both models, subsequent changes in the ν(OH) band shape during gelation can therefore be related to a change in the hydrogen bonding structure of associated water molecules. When the ratio of the single beam spectra for the copolymer solution and that of pure water at the same temperature is obtained, three possible types of behaviour may be observed.

1. Since the water concentration in the copolymer solution will always be lower than that of pure water and according

to the Beer–Lambert law the associated band intensity will be lower, a negative band [i.e. $\log(I_{wp}/I_w) < 0$] is anticipated.
2. If the water hydrogen bonding strength within the solution (or gel) is the *same* as that of pure water, then the band shape should be an inversion of the spectrum of pure water at a given temperature.
3. If the water hydrogen bonding strength within the solution (or gel) is *different* from that of pure water, then a more complex band shape is expected. Depending on their precise peak position, spectral features with a different intensity and lineshape than a simple inversion of the pure water band shape can therefore be related to weaker or stronger hydrogen bonding of associated water within the gel compared to pure water at the same temperature.

Fig. 2(c) shows that the high wavenumber component of the ν(OH) band increases relative to other components within the same band at higher temperature. Hence the average hydrogen bonding strength of water molecules within the gel decreases relative to the bands due to pure water on heating the copolymer solution. Thus water within the micellar gel is somewhat more weakly hydrogen-bonded than that of pure water at the same temperature, as expected given the amphiphilic nature of the PNIPAM–PMPC–PNIPAM triblock copolymer. This seems reasonable, since water within the copolymer gel is likely to contain a larger proportion of water molecules that are hydrogen-bonded to the MPC ester groups (rather than other water molecules) compared with the copolymer solution. Recent work by Sammon et al. has shown that these water–polymer interactions can have a significant effect on the shape of the water band [38]. Since there is an evolution of changing water band shapes above the critical gelation temperature, the water hydrogen bonding network must have a different structure in the copolymer gel compared to the aqueous copolymer solution prior to gelation. This suggests some degree of cooperation between the organisation of the copolymer chains and the associated water molecules.

To confirm the latter hypothesis, it is necessary to consider some of the bands associated with functional groups on the copolymer chains to see if it is possible to identify the cause of those differences. The ABA triblock copolymer comprises two PNIPAM blocks that can form hydrogen bonds with water via the NH and C=O groups of the amide groups and the PMPC block that can interact via its ester C=O groups. However, it is worth emphasising that only the two outer PNIPAM blocks actually become hydrophobic above the critical gelation temperature; the PMPC block is expected to remain hydrophilic regardless of the solution temperature. These three bands have different wavenumbers and are highly sensitive to local interactions. In principle, they can be highly informative regarding subtle changes in the water–polymer interactions that occur during gelation. Fig. 4(a) shows the band shape and position of the ester C=O as a function of temperature; these spectra were obtained by using the clean ATR crystal as a background reference. It is clear that the position of this band is unchanged during gelation, which implies that there

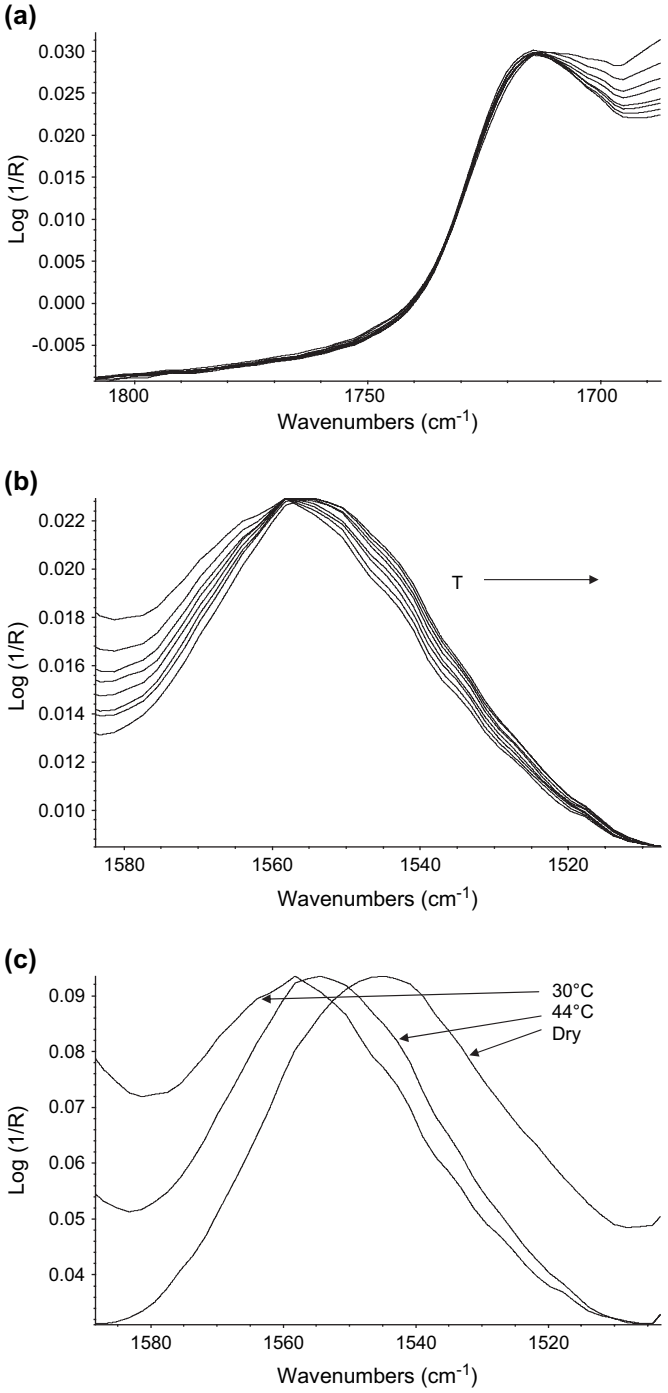

Fig. 4. Comparison of the NH amide I band recorded in (a) aqueous solution, (b) in the micellar gel and (c) for the dry $PNIPAM_{89}$–$PMPC_{250}$–$PNIPAM_{89}$ triblock copolymer.

is no change in the local environment of the ester groups associated with the central PMPC block during gelation, as expected. In contrast, Fig. 4(b) shows the changes associated with the amide II NH vibrations that correspond to the outer PNIPAM blocks. The amide II NH vibration at $\sim 1560\ cm^{-1}$ (see Fig. 4(b)) is clearly red shifted by increasing temperature. Any temperature dependence is less evident directly for the amide carbonyl band at $\sim 1650\ cm^{-1}$, due to its overlap with the δ(OH) vibration of water at $\sim 1625\ cm^{-1}$ some

deconvolution is required which will be discussed later. Comparing the position of the NH vibrational band in the solution, gel and dry states (see Fig. 4(c)), it is clear that there is a significant shift towards the dry state band position during gelation, which is a strong evidence for the selective dehydration of this block during the micellar network formation. It is important to note that heating the *solid* copolymer within this temperature range showed no evidence of any wavenumber shifts for the three bands under discussion. Similar shifts in the amide II band were also observed by Jaber and Schlenoff [39] in a layer-by-layer sequentially assembled PAH-*co*-PNIPAM/PSS-*co*-PNIPAM system and these shifts correlated well with changes in the degree of hydration monitored using the ν(OH) band of sorbed water.

Deconvolution of the bands in the 1800–1500 cm^{-1} region as a function of temperature is also instructive. This region is composed of four bands at ~1712 cm^{-1} (ester), ~1650 cm^{-1} (amide I), ~1625 cm^{-1} (water) and ~1560 cm^{-1} (amide II). Plotting the position of each of these bands against temperature leads to a better understanding of the water–copolymer interactions during gelation. Fig. 5 shows a typical fit obtained for the 1800–1500 cm^{-1} region of the copolymer spectrum using the clean, dry ATR crystal at the same temperature as a background reference; a plot of the peak position of each of these bands as a function of time is shown in Fig. 6. From the latter figure it is clear that both the water bending mode at ~1625 cm^{-1} and the ester carbonyl at ~1712 cm^{-1} only vary by 2 cm^{-1} on either side of the critical gelation temperature. The bending mode of liquid water is not particularly sensitive to changes in hydrogen bonding strength, as discussed previously and shown in Fig. 3(a). Thus this band is not expected to be particularly diagnostic with respect to the inherent changes in water–copolymer hydrogen bonding that must occur during gelation. The ester carbonyl of the PMPC block should be highly sensitive to changes in the local hydrogen bonding network [40–45]. Thus the lack of any significant changes in the position of this band during gelation indicates that the degree of hydrogen bonding between the water molecules and the central PMPC block is very similar in aqueous solution and in the gel phase. A shift in the ester band to lower wavenumber usually indicates an increase in the strength and/or number of hydrogen bonds, but a 2 cm^{-1} shift is perhaps small enough to be considered insignificant within the limits of the spectral resolution of 4 cm^{-1}. In contrast, the amide I and amide II bands shift by more than 4 cm^{-1} (to higher and lower wavenumbers, respectively) as the solution temperature is increased. These peak shifts indicate a reduction in hydrogen bonding between the water molecules and the amide groups of the PNIPAM blocks [34,45], which is consistent with the ^{1}H NMR studies reported by Li and co-workers for this triblock copolymer gelator [14]. It is particularly noteworthy that the changes in the position of the amide I band are most dramatic at around 32 °C, which corresponds to the approximate cloud point temperature of the PNIPAM chains. An obvious conclusion is that dehydration of the PNIPAM blocks plays an important role in the gel formation mechanism. The hydrophobic interactions between methyl groups on neighbouring polymer chains impart some reduction in chain mobility and hence play a role in the formation of the micellar network. Fig. 5(e) shows a plot of the change in wavenumber for the ν_{as}(CH) band as a function of temperature for both the heating and cooling cycles. As mentioned previously, the observed red shift is strong evidence of hydrophobic interactions between the dehydrated PNIPAM chains of the copolymer [32]. The largest wavenumber shift occurs just below the cloud point temperature (between 30 and 32 °C), which corresponds to the greatest change in the peak position of the amide I band, see Fig. 6(d). This indicates that hydrophobic interactions occur just prior to the dehydration of the PNIPAM blocks. Thus spectroscopic changes in the bands associated with two different functional groups of the same PNIPAM copolymer block provide strong evidence for the preferential dehydration of the PNIPAM blocks.

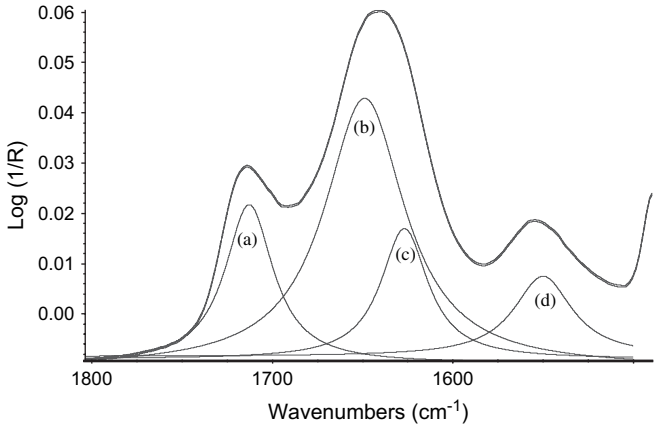

Fig. 5. Peak fitting of 100% Lorentzian line shapes to the (a) PMPC ester carbonyl, (b) PNIPAM amide I, (c) water bending mode and (d) PNIPAM amide II peaks of the copolymer gel at 44 °C.

Complementary information relating to the nature of hydrogen bonding can also be obtained by examining changes in the *intensities* of the water, ester, amide I and amide II bands. Numerous studies on carbonyl-containing molecules have shown that the ν(C=O) band intensity is sensitive to interactions with hydrogen bonding species [40–45]. Strong hydrogen bonding species can lead to an increase in the magnitude of the dipole moment change during the vibration, leading to more intense carbonyl bands, i.e. a larger molar extinction coefficient (ε). Fig. 7 shows the temperature dependence of the intensities of the water δ(OH), ester ν(C=O), amide I ν(C=O) and amide II b(NH) bands. The intensity changes of the water bending mode have already been explained in terms of water expulsion from between copolymer chains during the formation of the micellar gel network. The changes in the ester and amide carbonyls are also readily explained by relative changes in hydration. The amide I band shows a significant decrease in intensity at higher temperatures, which supports the earlier suggestion that hydrogen-bonded water is preferentially removed from the PNIPAM blocks. Moreover, there is a general trend for an increase in the intensity of bands associated with the copolymer backbone due to the higher density of the gel compared to the solution.

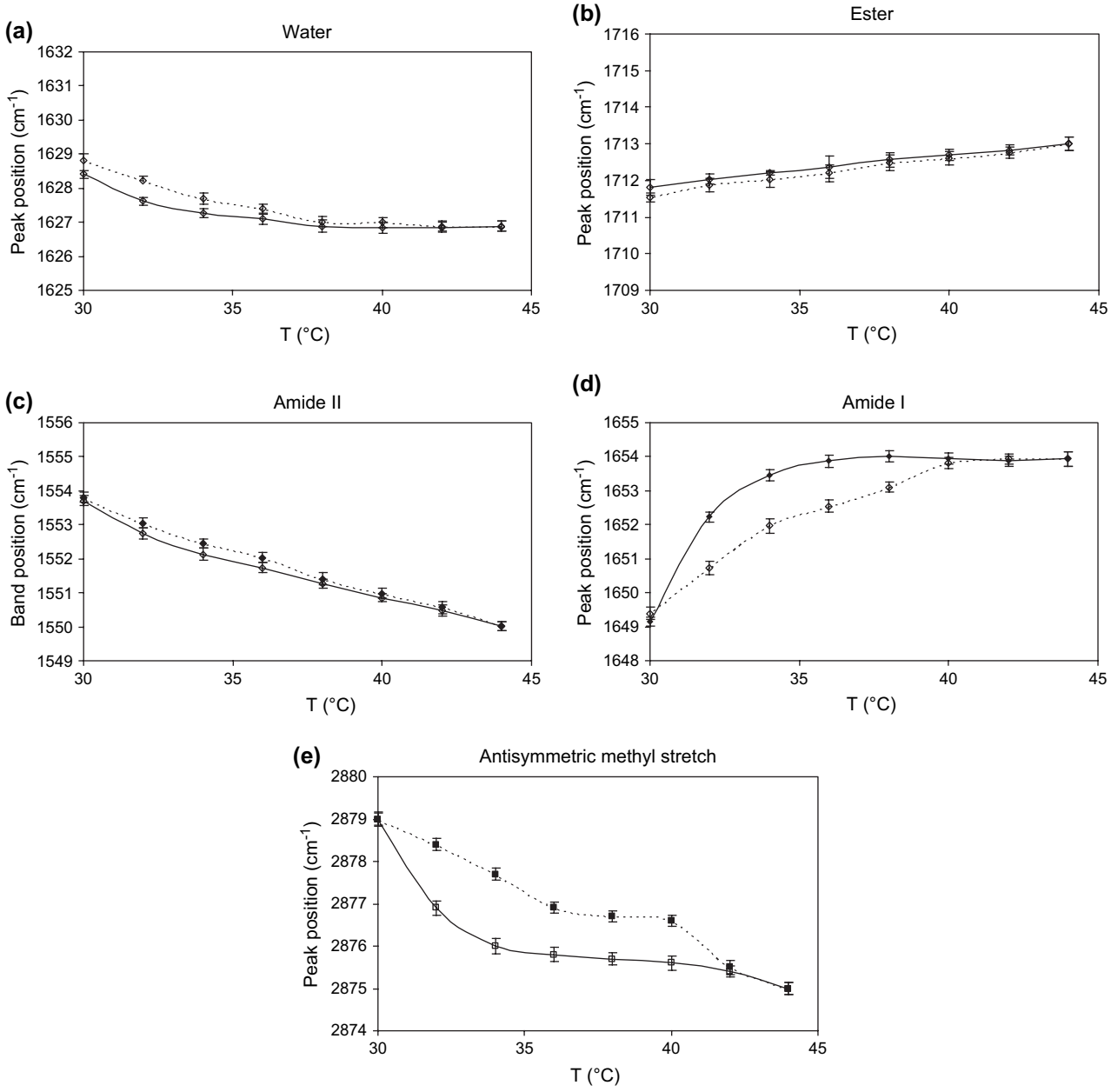

Fig. 6. Peak positions of the (a) water bending mode, (b) PMPC ester carbonyl, (c) PNIPAM amide II, (d) PNIPAM amide I and (e) the antisymmetric methyl stretch of the copolymer solution/gel as a function of temperature. The solid line denotes the heating cycle and the dotted line denotes the cooling cycle in each plot. The mean value of three measurements of the same stock solution is recorded, with the error bars representing one standard deviation from the mean value.

Thus the reduced intensity of the amide I band is partially offset by the higher copolymer concentration in the evanescent field. On the other hand, the amide II band shows little or no change in intensity with increasing temperature. However, we are not aware of any literature evidence to suggest that the band intensities of N–H stretching vibrations are as sensitive to changes in hydrogen bonding as carbonyl ester bands.

Figs. 6 and 7 also indicate some evidence of hysteresis during the heating and cooling cycles, which was also observed during heat capacity measurements on the same systems [46]. This suggests that there is a relationship between the observed spectroscopic changes and the heat capacity measurements, i.e. they are monitoring the same molecular event. In this case it is the selective dehydration of the PNIPAM chains followed by the formation of a micellar gel network. The hysteresis observation also points to a difference in the time dependence of the gelation and solvation phenomena that must be related to the mobility of the system. Ding et al. [47] have indicated that the hysteresis effects of the heating and cooling PNIPAM-based systems are likely to be due to the dissolution process consisting of two stages; (i) disruption of additional hydrogen bonding formed in the collapsed state and (ii) the subsequent dissolution of collapsed and entangled chains.

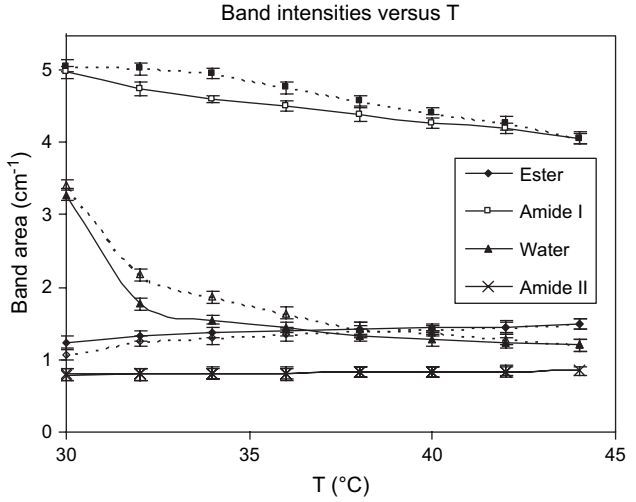

Fig. 7. Temperature dependence of the band intensities (solid lines heating, dotted lines cooling) for the δ(OH), ν(C═O), amide (I) and amide (II) modes. The mean value of three measurements of the same stock solution is recorded, with the error bars representing one standard deviation from the mean value.

4. Conclusions

Variable temperature ATR–FTIR spectroscopy has been used to elucidate molecular interactions during the thermoreversible gelation of an aqueous solution of a $PNIPAM_{89}$–MPC_{250}–$PNIPAM_{89}$ triblock copolymer. Various changes in band intensities, red shifts of the NIPAM amide I carbonyl band and blue shifts of the NIPAM amide II band, coupled with no significant changes in the MPC ester carbonyl peak position, are consistent with the preferential dehydration of the PNIPAM blocks during micellar network formation. Loss of water from *between* copolymer chains (i.e. syneresis) was detected by a reduction in the intensity of both the ν(OH) and δ(OH) bands of water during gelation. Red shifts in the peak position of the ν_{as}(CH) band indicated hydrophobic interactions between copolymer chains during the formation of the micellar network. The largest wavenumber shift of the ν_{as}(CH) band was observed between 30 and 32 °C, which was followed by the greatest red shift of the amide I peak at 32–34 °C. This is consistent with the preferential dehydration of the PNIPAM blocks during gelation.

References

[1] Heskins M, Guilet J. J Macromol Sci Chem 1968;A2:1441.
[2] Wu C, Wang X. Phys Rev Lett 1998;80:4092.
[3] Yoshida R, Uchida K, Kaneko Y, Sakai K, Kikuchi A, Sakurai Y, et al. Nature 1995;374:240.
[4] Yamada N, Okano T. Macromol Chem Rapid Commun 1990;11:571.
[5] Qiu Y, Park K. Adv Drug Deliv Rev 2001;53:321.
[6] Canavan HE, Cheng X, Graham DJ, Ratner BD, Castner DG. Langmuir 2005;21:1949.
[7] Sun T, Wang G, Fen L, Liu B, Ma Y, Jiang L, et al. Angew Chem Int Ed 2004;43:357.
[8] Hu Z, Chen Y, Wang C, Zheng Y, Li Y. Nature 1998;393:149.
[9] (a) Hayward JA, Chapman D. Biomaterials 1984;5:135;
(b) Durrani AA, Hayward JA, Chapman D. Biomaterials 1986;7:121;
(c) Lewis AL. Colloids Surf B Biointerfaces 2000;18:261;
(d) Murphy EF, Lu JR, Lewis AL, Brewer J, Russell J, Stratford P. Macromolecules 2000;33:4345.
[10] (a) Ishihara K. Trends Polym Sci 1997;5:401;
(b) Moro T, Takatori Y, Ishihara K, Konno T, Takigawa Y, Matsushita T, et al. Nat Mater 2004;3:829;
(c) Yusa S, Fukuda K, Yamamoto T, Ishihara K, Morishima Y. Biomacromolecules 2005;6:663.
[11] (a) Driver MJ, Jackson DJ. US Patent No. 5,741,923, Biocompatibles Ltd.; 1998.
(b) Uchiyama T, Watanabe J, Ishihara K. J Memb Sci 2002;208:39;
(c) Nam KW, Watanabe J, Ishihara K. Biomacromolecules 2002;3:100.
[12] Iwasaki Y, Nakabayashi N, Ishihara K. J Biomed Mater Res 2001;57:72.
[13] (a) Lobb EJ, Ma I, Billingham NC, Armes SP, Lewis AL. J Am Chem Soc 2001;123:7913;
(b) Ma I, Lobb EJ, Billingham NC, Armes SP, Lewis AL, Lloyd AW, et al. Macromolecules 2002;35:9306;
(c) Wang J, Matyjaszewski K. J Am Chem Soc 1995;117:5614;
(d) Matyjaszewski K, Xia J. Chem Rev 2001;101(9):2921.
[14] Li C, Tang Y, Armes SP, Morris CJ, Rose SF, Lloyd AW, et al. Biomacromolecules 2005;6:994.
[15] Bertie JE, Lan Z. Appl Spectrosc 1995;49(6):840.
[16] Libnau FO, Kvalheim OM, Christy A, Toft J. Vib Spectrosc 1994; 7(3):243.
[17] Libnau FO, Chrsty AA, Kvalheim OM. Appl Spectrosc 1995;49(10):1431.
[18] Hare DE, Sorensen CM. J Chem Phys 1992;96:13.
[19] Sammon C, Mura C, Yarwood J, Everall N, Swart R, Hodge D. J Phys Chem 1998;102:3402.
[20] Sammon C, Yarwood J, Mura C, Pereira M. J Mol Liq 1999;80:93.
[21] Hajatdoost S, Sammon C, Yarwood J. Polymer 2002;43:1821.
[22] Harrick NJ. Internal reflection spectroscopy. In: Harrick NJ, editor. New York: Harrick Scientific Corporation; 1987.
[23] Banks SR, Sammon C, Melia CD, Timmins P. Appl Spectrosc 2005; 59(4):452.
[24] Ostrovskii D, Kjoniksen A-L, Nystrom B, Torell LM. Macromolecules 1999;32:1534.
[25] Goeden-Wood NL, Keasling JD, Muller SJ. Macromolecules 2003; 36(8):2932.
[26] Gosal WS, Clark AH, Pudney PDA, Ross-Murphy SB. Langmuir 2002; 18(19):7174.
[27] Iizuka K, Aishima T. J Food Sci 1999;64(4):653.
[28] Bilkin BJ, Kwak Y, Dea ICM. Carbohydr Res 1987;160:95.
[29] Wilson RH, Belton PS. Carbohydr Res 1988;180:339.
[30] Liu Q, Charlet G, Yelle S, Arul J. Food Res Int 2002;35:397.
[31] Malik S, Nandi AK. J Phys Chem B 2004;108(2):597.
[32] Su YL, Liu HZ, Guo C, Wang J. Mol Simulat 2003;29(12):803.
[33] Su YL, Wang J, Liu HZ. Macromolecules 2002;35:6426.
[34] Maeda Y, Higuchi T, Ikeda I. Langmuir 2000;16:7503.
[35] Maeda Y, Nakamura T, Ikeda I. Macromolecules 2001;34:1391.
[36] Falk M. Symposium proceedings. Chem Phys: Aqueous Gas. NJ: Electrochemical Society Princeton; 1975, and references therein.
[37] Walrafen GE. Water, a comprehensive treatise. In: Franks F, editor. New York: Plenum Press; 1972. p. 208–9.
[38] Sammon C, Deng CS, Yarwood J. Polymer 2003;44:2669.
[39] Jaber JA, Schlenoff JB. Macromolecules 2005;38:1300.
[40] Paul SO, Ford TA. J Mol Struct 1989;198:65.
[41] Paul SO, Ford TA. J Chem Soc Faraday Trans 2 1981;77:33.
[42] Paul SO, Ford TA. Spectrochim Acta A 1988;44(6):587.
[43] Paul SO, Ford TA. J Mol Struct 1987;160(1–2):67.
[44] Tshehla TM, Ford TA. S Afr J Chem 1995;48(3–4):127.
[45] Galabov BS, Dudev T. Vibrational spectra and structure. In: Durig JR, editor. Amsterdam: Elsevier; 1996. p. 22.
[46] Li C, Buurma NJ, Haq I, Turner C, Armes SP, Castelletto V, et al. Langmuir 2005;21(24):11026.
[47] Ding Y, Ye X, Zhang G. Macromolecules 2005;38:904.